

## Identification of Wire Network Topology Using Impedance Spectroscopy

Qinghai Shi<sup>1</sup>, Olfa Kanoun<sup>1</sup>

<sup>1</sup> Chair for Measurement and Sensor Technology, Chemnitz University of Technology, Chemnitz, Germany,  
+49 371 531 37788, +49 371 531 837788  
[qinghai.shi@ieee.org](mailto:qinghai.shi@ieee.org), [Kanoun@ieee.org](mailto:Kanoun@ieee.org)

**Abstract-** A new technique is proposed to locate wire faults and identify wire network topology using impedance spectroscopy (IS). The propagation along the cables is analytical, modelled with flexible multi section cascading features utilizing frequency dependent scattering parameters. Therefore, it doesn't have the common numerical method problems. The transmission line model has the same spectrum as the measured reflection coefficient ( $\rho$ ) of wire under test (WUT) so that same practical effects such as skin and proximity effects, signal loss, dispersion and frequency dependent signal propagation can be exactly incorporated. For determination of model parameters an inverse problem should be resolved and differential evolution (DE) approach is proposed. The novel method allows locating hard (short and open circuit) and soft (frays and junctions) faults and also for characterization of defects in the branches of network. Results are presented to validate and illustrate the performance of this proposed method.

**Keywords-** Scattering parameters, reflection coefficient, Impedance Spectroscopy, global optimization technique, wire fault location, network topology.

### I. Introduction

The increasing use of the wiring in vehicles, communication and power systems has caused growing requirement for characterization of wire network and location of wire faults. The most widely used technique is reflectometry. Thereby, a high-frequency signal is sent down the cable. The reflected signal including information about changes of cable impedance is used to locate wiring faults. Over the last decade, many methods, such as Time Domain Reflectometry (TDR) [1], Frequency Domain Reflectometry (FDR) [2], Ultra Wide Band (UWB) based TDR [3], and Spectrum Time Domain Reflectometry (STDR) [4] were developed. They use different incident signal and signal processing methods. However, these techniques fail to detect soft faults such as frays or chafes and identification of the network topology in practice.

Some improved TDR methods use the baseline method, in which the output signal of the faulty wire is compared with the output of the healthy wire, in order to enable to detect and locate the soft faults. The TDR method has the advantage to identify the type of wire faults. Other methods focus more on improving location accuracy.

But for all these methods, knowledge of the wire material parameters should be known in advance and the excitation signal and its bandwidth should fulfil high quality requirements. This is because for fault localization, the time of flight is transformed to the location by means of the wave propagation velocity, which is dependent on the wire type and the available frequencies of the excitation signal.

Furthermore, soft faults, such as frays and chafes, and multiple faults are difficult to detect by the baseline method. Especially at higher complexity of the wire topology there are practical difficulties because of noise, multiple reflections, unknown load impedances, mechanical variations and changes of electrical parameters due to different wires types.

The aim of this study is that an automated method is developed for the location of hard and soft wire faults, identification of the type of wire faults and characterization of the network topology. In this study the propagation along the cables is analytical, modelled with flexible multi section cascading features using frequency dependent scattering parameters. It doesn't have the common numerical method problems for instance using finite element method (FEM) or finite difference in time domain (FDTD), in which the simulation time is linear or proportional to the wiring length and complexity of the transmission line systems. The same practical effects such as skin and proximity effects signal loss, dispersion and frequency dependent signal propagation can be exactly incorporated by the forward model. Therefore, this model is much more efficient, accurate than the numerical methods and is able to simulate the very tiny wire faults. The results shown good matching between simulation and measurement data and consequently the optimization technique has a fast convergence and best accuracy. For determination of model parameters an inverse problem should be resolved and differential evolution (DE) approach is proposed. The input reflection coefficient is measured to locate the wire faults and identify the types of wire faults.

## II. Transmission line Model

Model based system identification methods are used to reconstruct the transmission line parameters. These algorithms consist of two parts. The first part is forward modelling which is used to simulate the transmission line. Then optimized techniques are used to solve the inverse problems. The simulated result of the forward modelling is applied to compare with the measured data. If they match each other, the wiring system can be identified and the wiring parameters can be reconstructed so that the wiring faults can be detected and located.

In this study ABCD matrix and S parameters methods are used to simulate the transmission lines in frequency domain with frequency dependent parameters in order to solve the limitations of the time domain transmission line modelling. With these methods transmission lines can be directly simulated in the frequency domain with realistic results. The simulation time of this algorithm is independent of the wire length because it is an analytical solution and flexible multi section cascading features so that this method has higher efficiency for the simulation and better accuracy than the time domain transmission line modelling.

The input impedance of WUT is measured in frequency domain by Impedance Spectroscopy (IS). The ABCD model and S parameters have been setting as the same spectrum as the measured input reflection coefficient of the transmission line system using impedance spectroscopy so that there is good matching between simulation and measurement data and consequently the optimization technique has a fast convergence and best accuracy.

### A. ABCD Matrix and S parameters

Fig. 1.a) illustrates the cross section of a simple coaxial cable. The inner conductor has a radius  $a$ . The outer conductor (shield) has an inner radius  $b$  and thickness  $\Delta$ . The outer radius of the shield is  $c$ . Both of the conductors have the same electrical conductivity  $\sigma$ . The cable interior is filled with a lossy dielectric having a relative permittivity  $\epsilon_{rel}$ . The magnetic permeability is assumed to be that of free space  $\mu_0$ . The relative permittivity is assumed to be frequency dependent.

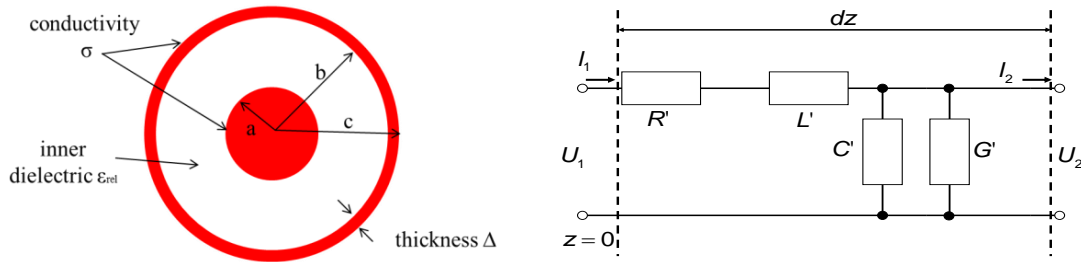


Figure 1.a) Cross section and b) Equivalent circuit of a coaxial cable per unit length

The per-unit-length line outer inductance parameter  $L'$  and capacitance parameter  $C'$  can be described by the following equations [5]:

$$L'_{out} = \frac{\mu_0}{2 \cdot \pi} \cdot \ln(b/a) \text{ H/m} \quad C' = \frac{2 \cdot \pi \cdot \epsilon_0 \cdot \epsilon_{rel}}{\ln(b/a)} \text{ F/m} \quad (1)$$

When the conductors of the coaxial line are finitely conducting, there will be additional per-unit-length impedance elements in the transmission line model that take into account both the magnetic flux penetration into the conductors and the resistive loss [5]. For the inner conductor with radius  $a$ , the per-unit-length impedance is given by following equation:

$$Z'_a(\omega) = \frac{\eta}{2 \cdot \pi \cdot a} \left[ \frac{J_0(\gamma \cdot a)}{J_1(\gamma \cdot a)} \right] \quad \Omega/\text{m} \quad (2)$$

Where  $J_0$  and  $J_1$  are modified Bessel functions of order zero and one.  $\omega$  is the angular frequency. The Term  $\eta$  is the wave impedance in the lossy conductor, and if the displacement current in the conductor is neglected, this term  $\eta$  and  $\zeta$  are given as:

$$\eta \approx \sqrt{\frac{j \cdot \omega \cdot \mu_0}{\sigma}} \quad \zeta = \sqrt{j \cdot \omega \cdot \sigma \cdot \mu_0} \quad (3)$$

The per-unit-length impedance of the outer shield is derived by following equation:

$$Z_b'(\omega) = \frac{\eta}{2 \cdot \pi \cdot b} \left[ \frac{J_0(\zeta \cdot b) \cdot K_1(\zeta \cdot c) + J_1(\zeta \cdot c) \cdot K_0(\zeta \cdot b)}{J_1(\zeta \cdot c) \cdot K_1(\zeta \cdot b) - J_1(\zeta \cdot b) \cdot K_1(\zeta \cdot c)} \right] \Omega/m \quad (4)$$

Where  $K_0$  and  $K_1$  are the modified Bessel functions of the second kind, and  $c$  is the outer radius of the shield. The transmission line model is composed of discrete resistors, inductors, capacitors and conductance. A length  $z$  of transmission line can conceptually be divided into an infinite number of increments of length  $\Delta z$  ( $dz$ ) such that series and shunt  $R'$ ,  $L'$ ,  $G'$  and  $C'$  are given as shown in Figure 1.b). Each of the parameters  $R'$ ,  $L'$  and  $G'$  is frequency dependent. For example,  $R'$  and  $L'$  will change in value due to skin effect and proximity effect.  $G'$  will change in value due to frequency dependent dielectric loss [5]. From equations (1)-(4) we can calculate the shunt  $R'$  ( $\Omega/m$ ),  $L'$  (H/m),  $G'$ (S/m) and  $C'$  (F/m):

$$R' = \text{real}[Z_a'(\omega) + Z_b'(\omega)] \quad L' = \text{imag}[Z_a'(\omega) + Z_b'(\omega)]/\omega + L_{\text{out}}' \quad (5)$$

$$G' = \frac{\pi \cdot \omega \cdot \varepsilon''}{\ln(b/a)} = \omega \cdot \tan \delta \cdot C' \quad C' = \frac{2 \cdot \pi \cdot \varepsilon_0 \cdot \varepsilon_{\text{rel}}}{\ln(b/a)} \quad (6)$$

Where  $\varepsilon''$  is the imaginary part of the complex permittivity and the  $\tan \delta$  is the dielectric loss tangent. The frequency dependency of the characteristic Impedance of a Transmission Line (TL)  $Z_0$  and the propagation constant of the transmission line with attenuation constant  $\alpha$  and phase constant  $\beta$  can be described by the following equations:

$$Z_0 = \sqrt{\frac{R' + j \cdot \omega \cdot L'}{G' + j \cdot \omega \cdot C'}} \quad \gamma = \alpha + j \cdot \beta = \sqrt{(R' + j \cdot \omega \cdot L') \cdot (G' + j \cdot \omega \cdot C')} \quad (7)$$

The impedance of a cable with length  $z$  and a certain load impedance  $Z_L$  is:

$$Z_{\text{in}}(z) = Z_0 \frac{Z_L + Z_0 \cdot \tanh(\gamma \cdot z)}{Z_0 + Z_L \cdot \tanh(\gamma \cdot z)} \quad (8)$$

The propagation in a coaxial cable can be modelled by RLGC parameters [5] in the frequency domain, as shown in Fig. 1.b).

$$U_1 = U_2 \cdot \cosh(\gamma \cdot z) + I_2 \cdot \Gamma \cdot \sinh(\gamma \cdot z) \quad I_1 = U_2 \cdot \sinh(\gamma \cdot z)/\Gamma + I_2 \cdot \cosh(\gamma \cdot z) \quad (9)$$

Then ABCD matrix with 2-port network is applied to describe the voltages and currents in the transmission line in equation (9).

$$\begin{Bmatrix} U_1 \\ I_1 \end{Bmatrix} = \begin{bmatrix} A & B \\ C & D \end{bmatrix} \cdot \begin{Bmatrix} U_2 \\ I_2 \end{Bmatrix} \quad (10)$$

ABCD matrix is preferred since the matrix representation of several cascaded networks is obtained by matrix multiplications. Each entry in the matrix is now an  $M \times M$  matrix, where  $M$  is the number of signal conductor. The ABCD matrix representation of  $N$  cascaded 2-port networks can be obtained by  $(N-1)$   $2 \times 2$  matrix multiplications. For this case, the ABCD matrix can be used to simulate multiple cascaded transmission line and load discontinuities [6].

With the equations (8) and (10) the input impedance of cable can be written as:

$$Z_{\text{in}} = \frac{A \cdot Z_L + B}{C \cdot Z_L + D} \quad (11)$$

Then the input impedance of wiring system with wiring faults can be calculated by the ABCD matrix of the wiring system.

If the inner impedance of source equals the characteristic impedance of cable, the scattering parameter  $S_{11}$  at the input of cable system can be given as [6]:

$$S_{11}(f) = \frac{Z_{in} - Z_0}{Z_{in} + Z_0} = \rho_L \cdot e^{-2\gamma z} = \rho_{in} \quad (12)$$

Where  $\rho_L$  is the reflection coefficient at the load discontinuity,  $z$  is the cable length and  $\rho_{in}$  is the reflection coefficient at the input of cable. From the equation (12) we can see that if the source impedance matches the characteristic impedance of cable, the scattering parameter  $S_{11}$  has the same value with the reflection coefficient at the input of cable system.

### B. Comparison between Simulation and Measurement

In this work a typical coaxial cable RG58 C/U is used for the estimation. The radius of inner conductor is  $a = 0.508$  mm, the radius of the dielectric insulation is  $b = 2.000$  mm, the outer radius of shield is  $c = 2.200$  mm, the dielectric permittivity is  $\epsilon_{rel} = 2.25$ , the dielectric loss tangent  $\delta = 10^{-4}$  and the conductivity of both conductors is  $\sigma = 58.13 \cdot 10^6$  S/m.

A commercial impedance spectroscopy Agilent 4294a and Test Fixture 16047E are applied to acquire the input reflection coefficient of the coaxial cable in the frequency domain from 1 kHz to 110 MHz.

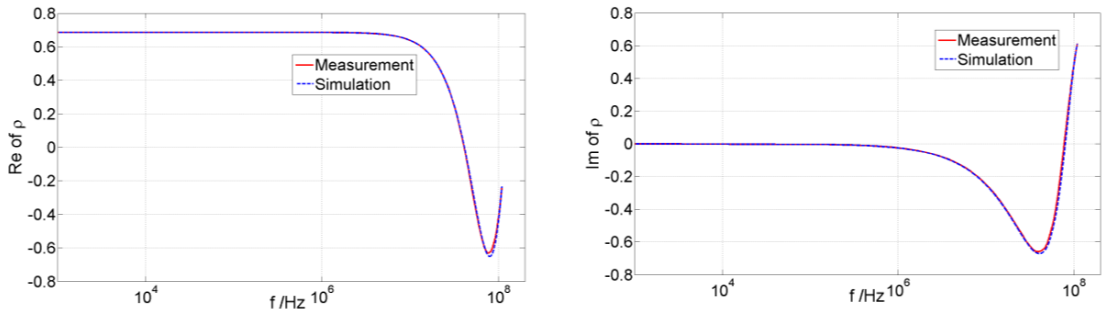


Figure 2. Comparison between simulation and measurement of the real and imaginary part of the reflection coefficient of a coaxial cable system with a length of 0.62m and load impedance of 270Ω

Fig. 2 presents a comparison between simulated and measured real and imaginary part of the reflection coefficient  $\rho_{in}$  of the studied coaxial cable with a length of 0.62m and load impedance of 270Ω. The figure shows the good matching between theory and experiment. The maximal error between simulated and measured result is less than 2% over the entire measured frequency range from 1 kHz to 110 MHz.

### III. Parameter Extraction

In this study the measured and simulated data of the input reflection coefficient of a coaxial cable in the frequency domain are applied to locate wire fault and identify the type of wire fault. The global optimization technique DE is applied to solve the inverse problem because of its good performance of the minimum-seeking and an efficient working with numerically experimental data [7].

The fitness function of differential evolution in this study is given by (13), where  $\rho_M$  is the measured reflection coefficient of the coaxial cable,  $\rho_S$  is the simulated input reflection coefficient of the coaxial cable,  $df$  is the frequency step,  $BW$  is the bandwidth of the incident sinusoid signals and  $N$  is the number of the frequency of the input impedance matrix of the coaxial cable.

$$F\{z, Z_L\} = \sqrt{df / BW \cdot \sum_{n=1}^N \left( \frac{|\rho_M\{f_n\}| - |\rho_S\{f_n, z, Z_L\}|}{|\rho_M\{f_n\}|} \right)^2} \quad (13)$$

Where  $z$  is the length between wire fault and input source point,  $f_n$  is the frequency of the incident signal, and  $Z_L$

is the impedance of wire fault.

There are many local minimization values of this fitness function because of its non-linearity. Finding the minimum of a nonlinear function is especially difficult. Typical approaches to solve problems involve either linearizing the problem in a very confined region or restricting the optimization to a small region. In short, the constrained parameters are necessary for the quick convergence to find the minimum cost of fitness function. In this study we define the impedance of wire fault changing from  $0\Omega$  to  $2 \times 10^6\Omega$  and the wiring length changing from 0.1 m to 120.1 m. Consequently the minimum cost of  $F\{z, Z_L\}$  can be efficiently located. The mutation factor  $F$  in this study is 2 and the probability CR is 1. The size of population is 40.

#### IV. Results and Analysis

As an example, the estimation procedure is applied to simultaneous retrieve the two parameters  $z$  and  $Z_L$  from measured amplitude of input reflection coefficient of a cable system collected from a 2.1- and 100.1-m-long RG58 C/U coaxial cable with different load impedances.

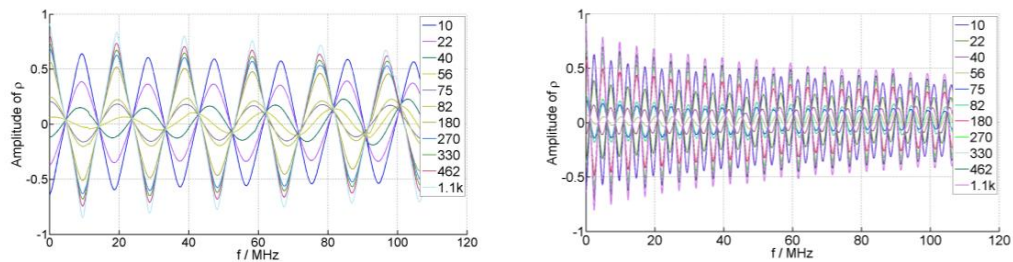


Figure 3. The input reflection coefficient a) of a 5.1-m-length coaxial cable with different load impedances, b) of a 20.1-m-length coaxial cable with different load impedances

Fig. 3 shows the number of period in waveform of the amplitude of the cable's input reflection coefficient is proportional to the distance to the fault. The peaks in Fig. 3.b are smaller for longer cables because of attenuation and dispersion.

The measurement deviation for wire fault location depends on the step frequency of the input signals  $\Delta f$  and the load impedance.

Fig. 4.a shows the behaviour of the absolute deviation of the wire fault location. The maximal absolute deviation is about 30 cm for different cable lengths. It can be optimized by the setting new step frequency of the input signals  $\Delta f$ . The larger  $\Delta f$  is, the smaller is the absolute error for wire fault detection. Therefore Fig. 4.a shows that the absolute deviation is relatively constant over the lengths estimation from 2.1 m to 100.1 m. This is independent of cable length.

If the load impedance of wire fault closely matches the characteristic impedance of the coaxial cable ( $50\Omega$ ), the measurement system has the maximal deviation (Fig. 4.b).

The results show an excellent reproducibility and a fast processing time which is less than 30 s for a cable with only a single fault.

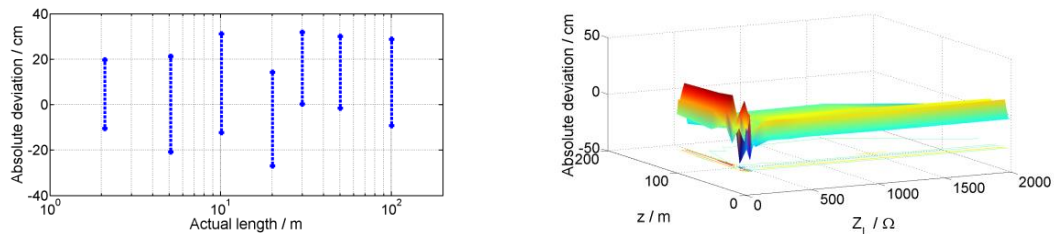


Figure 4.a) reconstruction accuracy of wire fault location of the coaxial cable, b) reconstruction accuracy of load impedance of the coaxial cable

The wire faults in the branches of network have been also in this study investigated. In this case the optimized parameters are the lengths of the different branches of the network and the impedance of the wire faults  $F\{z_i, Z_{L_j}\}$ . The faulty wiring network shows in Fig. 5. The mutation factor  $F$  in this example is 0.9 and the probability CR is 0.5. The size of population is 80. Fig. 5.b shows the reconstructed wiring network which has good matching with the original network. Fig. 6 shows also the comparison of the normalized amplitude of the input

reflection coefficient of the wiring network of forward and inverse model. The reconstructed wiring network has good matching to the original structure.

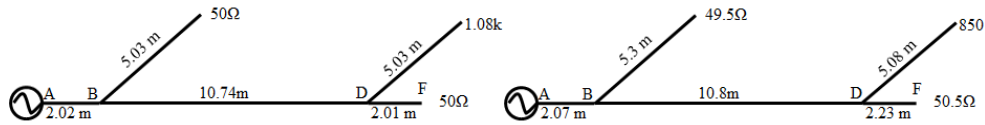


Figure 5. a) The studied (left) and b) reconstructed (right) wiring network topology and wire faults

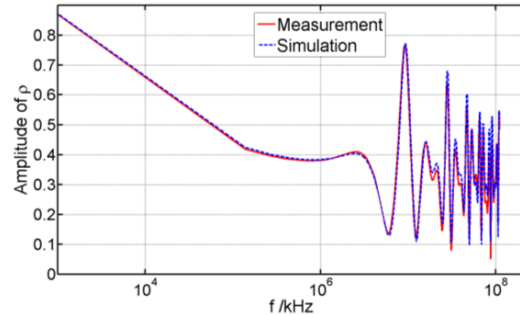


Figure 6. Amplitude of input reflection coefficient ( $\rho_{in}$ ) of the wiring network topology

## V. Conclusions

We proposed a generalized measurement method based on IS measurement and optimization techniques for location of the hard and soft wire faults, identification of the type of wire faults and characterization of the wire network topology. The efficient and accurate transmission line model using frequency dependent scattering parameters is applied for the forward model. The forward model of system structure is accurately represented as the actual hardware measured input reflection coefficient of the cable system in the simplest way. Finally, the inverse approach is easily generalized to handle the parameters of forward model and locate the wire faults and characterization of the wire network topology.

## References

- [1] Q. Shi, U. Troeltzsch, and O. Kanoun, "Analysis of the parameters of a lossy twisted-pair cable for cable fault location", *Transaction on Systems, Signals, and Devices*, vol. 7, No. 4, pp. 311-325, 2012.
- [2] Q. Shi, U. Troeltzsch, and O. Kanoun, "Detection and localization of cable faults by time and frequency domain measurements systems", *7th International Multi-Conference on Systems, Signal and Devices*, 2010.
- [3] C. Buccella, M. Feliziani, and G. Manzi, "Detection and localization of defects in shielded cables by time-domain measurements with UWB pulse injection and clean algorithm post processing", *IEEE Transaction on Electromag. Compat.*, vol. 46, pp. 597-605, 2004.
- [4] P. Smith, C. Furse, and J. Gunther, "Analysis of spread spectrum time domain reflectometry for wire fault location", *IEEE Sensors Journal*, vol. 5, pp. 1469-1478, 2005.
- [5] A. Schelkunoff, "The electromagnetic theory of coaxial transmission lines and cylindrical shields", *Bell Syst. Tech. J.*, pp. 532-579, 1934.
- [6] Q. Shi, and O. Kanoun, "System simulation of network analysis for a lossy cable system", *9th International Multi-Conference on Systems, Signal and Devices*, 2012.
- [7] K. V. Price, R. M. Storn and J. A. Lampinen, "Differential Evolution: A practical approach to global optimization", *Springer*, 2005.